Hindawi
Journal of Nanomaterials
Volume 2021, Article ID 5598924, 18 pages
https://doi.org/10.1155/2021/5598924

Research Article

Photoassisted Synthesis of Silver Nanoparticles Using Riceberry Rice Extract and Their Antibacterial Application

Pimsumon Jiamboonsri[1] **and Sompit Wanwong**[2]

[1]*Faculty of Medicine, King Mongkut's Institute of Technology Ladkrabang, Bangkok 10520, Thailand*
[2]*Materials Technology Program, School of Energy, Environment and Materials, King Mongkut's University of Technology Thonburi, Bangkok 10140, Thailand*

Correspondence should be addressed to Pimsumon Jiamboonsri; pimsumon.ji@kmitl.ac.th

Received 12 February 2021; Accepted 30 June 2021; Published 19 July 2021

Academic Editor: P. Davide Cozzoli

The green synthesis of silver nanoparticles (AgNPs) has been attractive in biomedical applications due to its nontoxic and eco-friendly approach. This study presents the facile, rapid, and cost-effective synthesis of AgNPs by photoassisted chemical reduction using Riceberry (RB) rice extract as a reducing agent. The effects of reaction parameters including photoirradiation, irradiation time, the volume ratio of silver nitrate ($AgNO_3$) to RB extract, and pH condition on the AgNP formation were also investigated. The characterization of AgNPs was determined by UV–visible spectroscopy, scanning electron microscopy (SEM), X-ray diffraction (XRD), and Fourier-transform infrared (FT-IR) spectroscopy. For antibacterial application, the synthesized AgNPs were studied by disc diffusion method against *Escherichia coli* and *Staphylococcus aureus*. The results indicated that light irradiation was an important factor to accelerate the formation of AgNPs. The synthesis parameters including volume of RB extract and pH condition significantly affected the particle size and crystallinity of AgNPs. The volume ratio of $AgNO_3$ to RB extract 1 : 12.5 at pH 2.5 under photoirradiation was the successful condition to form nanometer-sized crystalline particles (average particle size of 59.48 ± 0.37 nm) within 30 min with a rate constant of $0.210\ \text{min}^{-1}$. The FT-IR measurement also suggested that the phytochemical constituents in RB extract were served as reducing and stabilizing agents for the synthesis of AgNPs. Additionally, the obtained AgNPs from various conditions demonstrated the antibacterial activity against both strains. Therefore, this study proposes an effective integration technique to synthesize AgNPs within a short time for antibacterial application.

1. Introduction

In the past decade, nanoparticles (NPs), which are defined as particles having one or more dimensions between 1 and 100 nanometers (nm), have become popular in a wide range of application areas such as engineering [1], food [2], cosmetic [3], and textile [4, 5], as well as pharmaceutical field [6]. Among the metal NPs, silver NPs (AgNPs) is commonly used as an active antibacterial agent in medical applications [7], because the nanosize of Ag exhibits unique physico-chemical characteristics related to the improvement of anti-bacterial activity [8]. In addition, AgNPs can be used as a coating material on hospital textile, catheter, and implantable materials to prevent microbial infection [9]. However, these applications depend on the size and shape of AgNPs, and minimizing toxic residue from synthesis methods needs to be concerned [10, 11].

To date, synthesis of AgNPs can be achieved by physical [12], chemical [13], biological [14, 15], and hybrid methods [16]. The chemical-based synthesis by organic and inorganic reducing agents is the most common approach because it offers the reliability of large-scale production and short time synthesis [9, 14, 17]. However, a major drawback of chemical reduction is the use of toxic-reducing agents, such as sodium borohydride, trisodium citrate, and ascorbate, which produce hazardous wastes and greatly limit their biomedical applications [18]. Therefore, the biogenic synthesis of AgNPs using bacteria, algae, fungi, and plants has been attractive due to its

nontoxic and eco-friendly method. The utilization of plant-based synthesis provides advantages over a microorganism-based approach because it is a simple, easy scale-up, cost-effective, and nonaseptic process [19]. In comparison to microbial synthesis, a phytochemical synthesis can also produce AgNPs faster [20], and the formation of the metallic NPs is more stable without organic impurity produced by microorganisms [20, 21]. The extracts of edible and nonedible plants from various parts including roots of *Zingiber officinale* [22], stem bark of *Diospyros montana* [23], leaves of *Ziziphus mauritiana* [24], flowers of *Cassia angustifolia* [25], fruits of *Cordia dichotoma* [26], and seeds of *Psoralea corylifolia* [27] have been used for AgNP synthesis. Regarding phytomolecules, the polyol heterocyclic compounds of the plant extract serve as a reducing agent to convert silver ion (Ag^+) to AgNPs, whereas the flavonoid and terpenoid compounds act as a capping agent to stabilize AgNPs [28, 29]. Therefore, polyphenol-rich plants are a good alternative source to synthesize AgNPs.

Thai pigmented rice, namely, Riceberry (*Oryza sativa* L.), has been recently developed from a crossbreed strain of Hom Nin rice and Khoa Dawk Mali 105 for nutritional purposes. The purple rice barn extracts have been reported to have antioxidants, anti-inflammatory, anticancer [30], and antidiabetic activities [31]. The major constituents in a crude extract of RB bran are phenolic compounds [32], which possess hydroxyl (–OH) and carboxyl (–COOH) groups. These functional groups are capable of reducing the Ag^+ in an aqueous solution to form metallic silver. In addition, RB rice is commonly available in supermarkets all year round, inexpensive, no toxicity, and environment-friendly. Based on these reasons, RB rice extract becomes a potential agent for the production of nanomaterials. However, studies on the synthesis of AgNPs using different parts of nonpigmented and pigmented rice are limited. Utilizing rice bran, rice husk, rice germ, and rice leaf from the nonpigmented cultivar as a reducing agent could produce AgNPs with an approximate size range of 15–346.4 nm [33–35]. The differences in size, size distribution, and shape of AgNPs are affected by plant variety, plant parts, and synthesis conditions [36]. In addition, the optimal reaction time for AgNP synthesis using rice extract required at least an hour to complete the reaction at room temperature [35]. Therefore, it is necessary to consider the combination technique for reducing reaction time at room temperature and determine the factors influencing AgNPs synthesis utilizing Thai RB rice.

Recently, photoirradiation from UV light (or sunlight) has been employed to accelerate the formation of nanoparticles [37, 38]. However, few studies have reported the synthesis of AgNPs by incorporating light energy and plant-based reducing agent [39, 40]. Therefore, the objective of this study was to develop AgNPs by a combination technique using RB rice extract and photoirradiation. The effects of experimental parameters including photoirradiation, irradiation times with the kinetic reaction, volume ratio of $AgNO_3$ to rice extract, and pH conditions were also determined to identify desirable conditions. The obtained AgNPs have been characterized by using UV–Vis spectroscopy, SEM, XRD, and FT-IR, respectively. For the antibacterial application, the AgNPs were investigated by a disc diffusion method against both Gram-positive and Gram-negative bacteria.

2. Materials and Methods

2.1. Materials. The analytical grade of $AgNO_3$ (99%, purity) was purchased from Merck, Germany. Commercial RB rice (Hong Thong Life Riceberry Rice®) was purchased from a supermarket, Thailand. Hydrochloric acid (HCl) was purchased from J.T. Beker, USA. Sodium hydroxide (NaOH) was purchased from Merck, Germany. Analytical grade solvents including hexane, ethanol, and isopropanol were purchased from Fisher Scientific. Deionized (DI) water was used throughout the experiments.

2.2. Preparation and Standardization of RB Extracts. The rice grains (100 g) were extracted using 1% *v*/*v* HCl in DI water and ethanol at the ratio of 1 : 3 *w*/*v* for 12 h at 30°C. Then, the grains were extracted thrice with the same procedure. The obtained extract was defatted twice with hexane (1 : 1 *v*/*v*). Then, the aqueous extract was separated from the nonpolar part and filtered through a filter paper (Whatman® No.1, Merck, Germany), and subsequently, rotary evaporated under reduced pressure at 45°C. After the alcoholic solvents were evaporated, the remaining aqueous residue was freeze-dried to generate an RB extract with a yield of 3.62% *w*/*w* (on the basis of dry weight). The total phenolic content of the extract was analyzed using the Folin-Ciocalteu colorimetric method [41]. The RB extract was found to contain 12.94 ± 0.19 mg/g of total phenolic compounds expressed as the gallic acid equivalent (GAE, mg/g of extract).

2.3. Synthesis of AgNPs. AgNPs were prepared by a light-assisted chemical reduction method. First, $AgNO_3$ solution (50 mM) was mixed with 0.1% *w*/*w* of RB extract. After sonication for 5 min in an ice bath, the solution was irradiated by simulated sunlight under 1 sun (1.5 AM, 1,000 W/m^2, Newport 91150 V solar simulator) for 30 min at room temperature. The dispersed AgNPs were centrifuged and washed with DI water at 6,000 rpm for 30 min. The washing step was repeated 5 times to remove unreacted substances. The AgNPs were finally rinsed with isopropanol before drying in a vacuum oven at 40°C overnight. The effects of photoirradiation, irradiation times, volume ratios of $AgNO_3$ to extracted RB solution, and pH conditions were systematically investigated.

2.3.1. Effect of Photoirradiation, Irradiation Time, and the Kinetic of Reaction. The effect of irradiation light was observed under light irradiation and dark condition for 30 min by repeating the above procedure using the volume ratio of $AgNO_3$ to extracted RB at 1 : 12.5 and the pH condition of 2.5. The kinetic profile of photocatalytic reaction was investigated for 180 min. Then, the effect of irradiation time on the size and shape of AgNP was also studied.

2.3.2. Effect of Volume Ratio between $AgNO_3$ and Extracted RB Solution. To evaluate the effect of volume ratio, six different proportions of $AgNO_3$ to RB solution (3 : 1, 1 : 1, 1 : 3, 1 : 5, 1 : 7, and 1 : 10) were determined by repeating the above

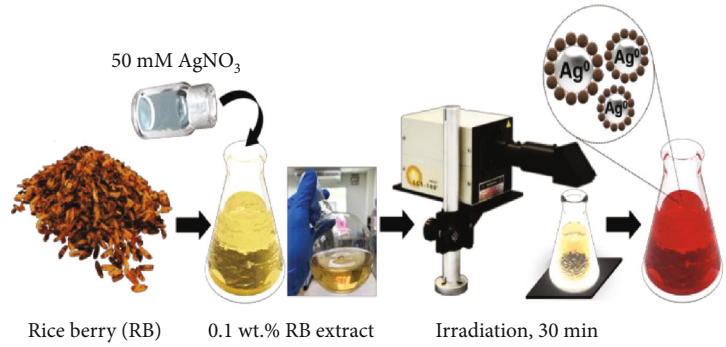

Figure 1: Schematic of green synthesis of AgNPs using RB extract under photoirradiation.

synthesis using a fixing pH condition of 2.5 and irradiation time of 30 min.

2.3.3. Effect of pH. The effect of pH conditions on the synthesis of AgNPs was investigated at pH values of 3, 5, 7, 9, and 11. The volume ratio of $AgNO_3$ to RB extract was 1 : 12.5, and the irradiation time was 30 min.

2.4. Characterization of Synthesized AgNPs. The optical property of synthesized AgNPs was determined by a UV–Vis spectrophotometer (Thermo Scientific UV–Genesys 10s). UV spectral analysis was studied in the range from 300 to 800 nm. Morphology of synthesized AgNPs was conducted through SEM (FEI Nova Nanosem 450). The average size of AgNPs was obtained from the particle size distribution carefully measured from the FE-SEM image. The particle size of Ag NPs was determined by the image processing in ImageJ software. By using "Analyze Particles," the automatic measurement of the area of each AgNP was obtained. The average diameter of each particle was calculated by using $A = \pi D^2/4$, where A is the area of AgNPs derived from ImageJ software and D is the average diameter of AgNPs. The crystal structure of synthesized AgNPs was investigated using an X-ray diffractometer (Bruker D8 ADVANCE diffractometer) operating at 40 kV and 40 mA with CuK_α radiation. XRD pattern of AgNPs recorded in the 2θ range from 20° to 80°. The average crystallite size of synthesized AgNPs was evaluated by using Scherrer's formula (as shown in Equation (1)).

$$D = \frac{K\lambda}{\beta \cos\theta}, \quad (1)$$

where D: the crystallite size

K: the dimensionless shape factor (0.9)

λ: the X-ray wavelength (1.5418 Å for CuK_α)

β: the line broadening at half the maximum intensity (FWHM) (radian)

θ: the Bragg angle (radian).

The functional groups present in RB extract and AgNPs derived by RB extract were analyzed by using FT-IR spectrophotometer (Thermo Scientific, Nicolet 6700 spectrophotometer). The spectra were recorded over the range of 400–4000 cm^{-1}.

2.5. Antibacterial Activities of AgNPs. S. aureus ATCC 25923 (Gram-positive bacteria) and *E. coli* ATCC 25922 (Gram-negative bacteria) were grown separately on Muller Hilton broth (Becton Dickinson & Co., France) at 37°C for 18–24 h. The bacterial-suspension turbidity was adjusted spectrophotometrically at 600 nm to obtain an optical density (OD) of 0.2, which contained approximately 10^7 colony-forming units (CFU)/mL, before use as inoculum in the antibacterial activity test. The antibacterial activities of AgNPs were evaluated against *S. aureus* and *E. coli* by the disc diffusion method [42]. Briefly, each prepared inoculum was swabbed on Mueller-Hinton agar (Becton Dickinson & Co., France) and air-dried at room temperature (25°C). The 6 mm sterile discs were loaded with 10 μL of AgNPs (20 mg/mL) placed on the agar plate. The plates were then incubated at 37°C for 24 h under aerobic conditions. The $AgNO_3$ solution (50 mM) and DI (10 μL/disc) were used as positive and negative controls, respectively. All disc diffusion tests were performed in triplicate, and the antibacterial activity was expressed as the mean of the inhibition diameter (mm) ± standard deviation (S.D.).

2.6. Statistical Analysis. All statistical analyses were carried out using IBM SPSS (version 26.0 for Mac). Analysis of variance was performed by ANOVA. Significant differences between the means were determined using Tukey's pairwise comparison test at a significance level of $p < 0.05$.

3. Results and Discussion

3.1. Synthesis of AgNPs Using RB Extract under Photoirradiation. AgNPs were successfully synthesized by irradiating the simulated sunlight to the solution of $AgNO_3$ (50 mM) and RB extract (0.1% w/w in DI water) (as illustrated in Figure 1). After light irradiation, the color of the solution was changed from white turbid to dark red within 5 min suggesting that Ag^+ was reduced to metallic Ag (Ag^0). On the other hand, the AgNPs from preliminary experiment were gradually formed within 60 min at pH 7 without sun irradiation. This suggested that photoenergy can accelerate chemical reduction process.

3.1.1. Effect of Photoirradiation on the AgNP Synthesis and the Kinetic of Reaction. To confirm the effect of

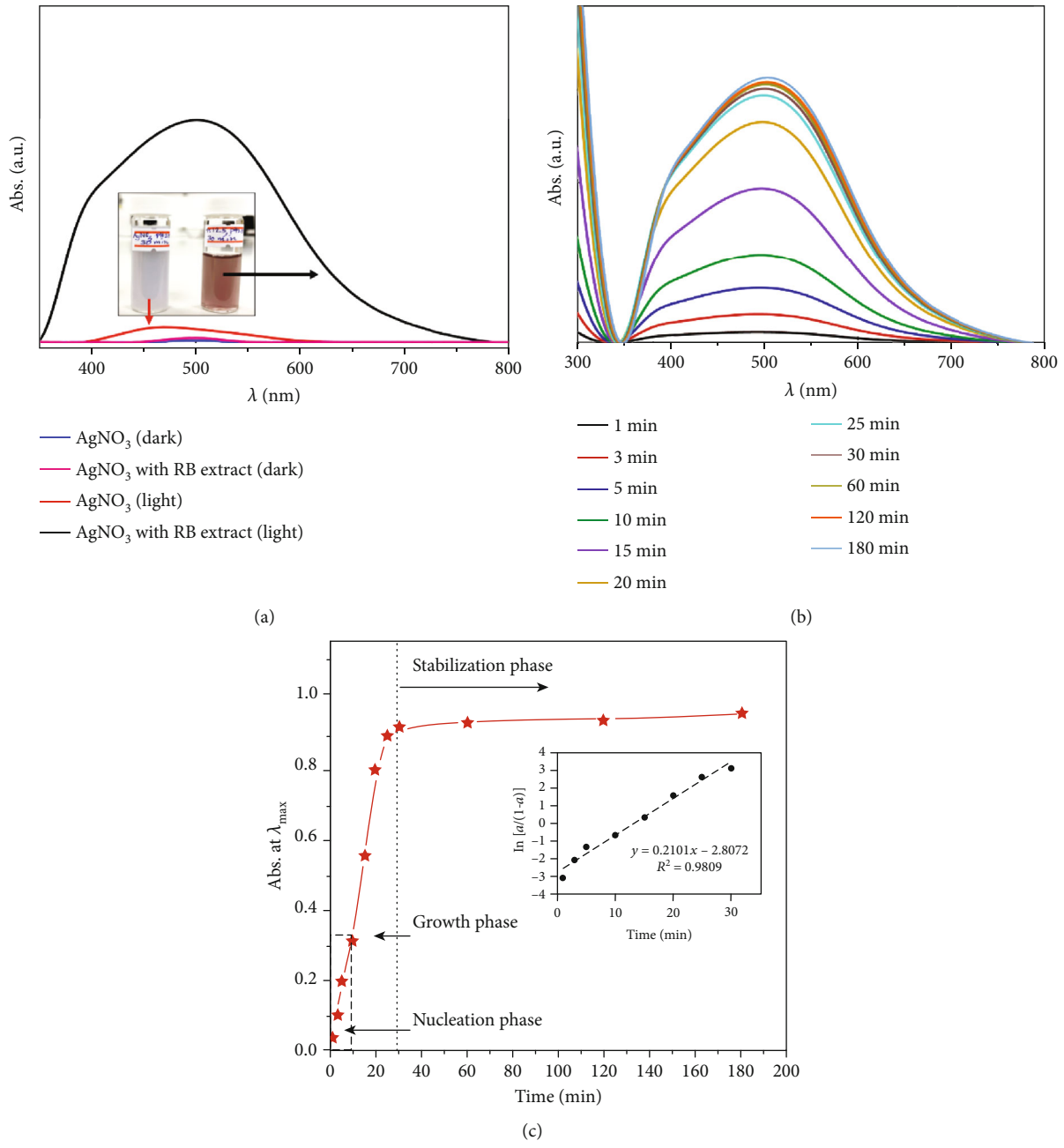

FIGURE 2: (a) Effect of irradiation light on the synthesis of AgNPs with and without RB extract ($AgNO_3$: RB extract 1 : 12.5, pH 2.5), (b) UV–vis spectra of AgNPs derived by various irradiation time from 1 to 180 min (b), and (c) kinetic of the synthesis of AgNPs plotting at maximum wavelength (500 nm) vs. irradiation time ($AgNO_3$: RB extract 1 : 12.5, pH 2.5).

photoirradiation on AgNPs production, fixing conditions with and without the presence of RB extract ($AgNO_3$: RB extract; 1 : 12.5) at pH 2.5 were observed under light irradiation comparing to the dark condition. The UV–vis technique was utilized to investigate the effect of RB extract on the formation of AgNPs. After 30 min of photoirradiation, the $AgNO_3$ solution with RB extract clearly showed the formation of AgNPs in dark red color solution with high absorption peak (Figure 2(a), black line), whereas the absorption band of $AgNO_3$ without RB extract showed significantly lower intensity than that of the $AgNO_3$: RB extract solution (Figure 2(a), red line). On the contrary, no absorbance peak was observed in both $AgNO_3$ solution with and without RB extract under the dark condition (pink and blue lines, respectively), indicating no AgNP formation. These results suggested that direct irradiation of light onto the silver solution was slightly influenced on AgNP formation or crystal growth process of Ag^0. In contrast, the incorporating light and RB extract acting as a reducing agent in the solution system can strongly induce the formation of AgNPs.

The kinetic of AgNP synthesis was also investigated by using the $AgNO_3$: RB extract ratio of 1 : 12.5 and pH 2.5

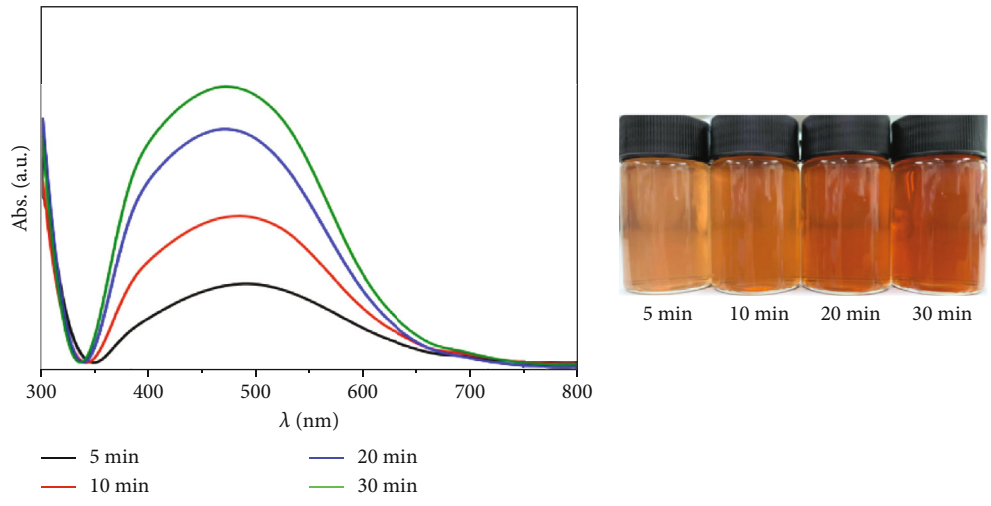

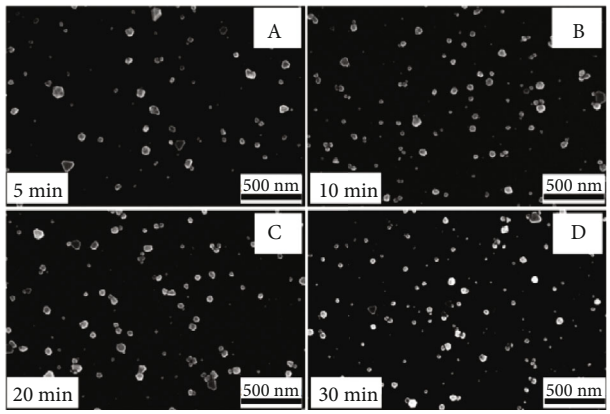

Figure 3: Continued.

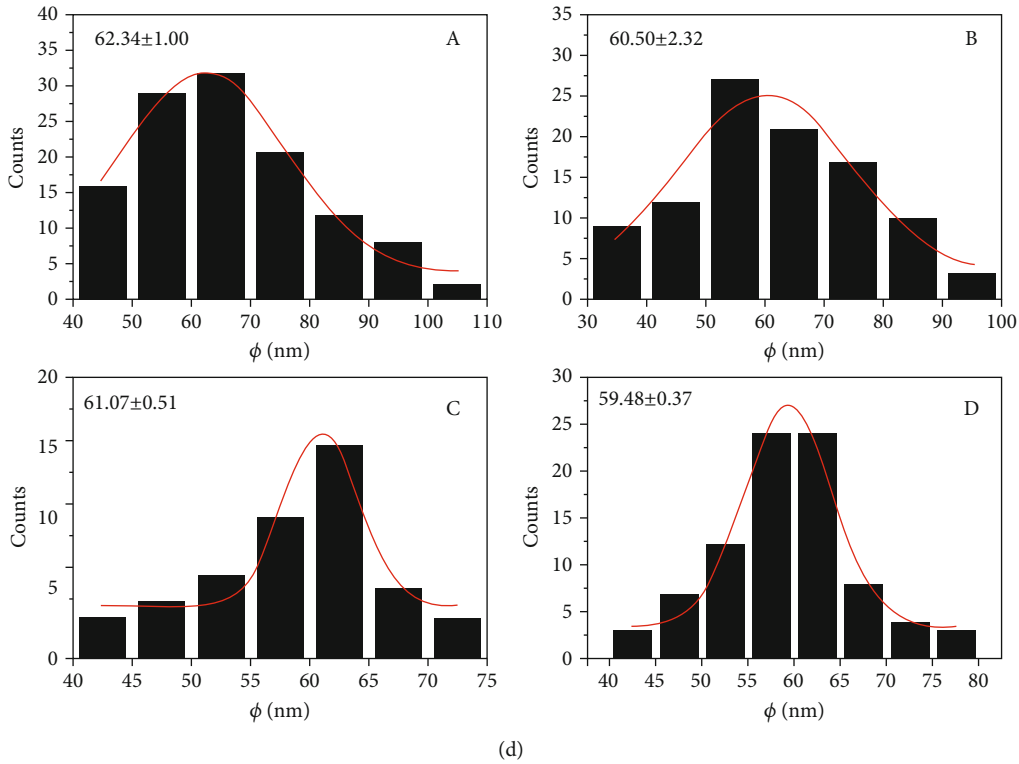

Figure 3: Effect of different irradiation times: A 5 min, B 10 min, C 20 min, and D 30 min ($AgNO_3$: RB extract 1 : 12.5, pH 2.5) on the characteristics of AgNPs: (a) UV–vis spectra, (b) the color of AgNPs dispersed in solution, (c) SEM images, and (d) particle size distribution.

under photoirradiation for 180 min. Figure 2(b) shows the UV–vis spectra of AgNPs suspended in the synthesized solution with different exposure times. As displayed in Figure 2(c), the kinetic graph demonstrated the sigmoid nature, which was characterized as autocatalysis [43]. The reaction demonstrated that the seed particles were formed within the first 10 min of the reaction (nucleation phase), followed by a rapid growth phase to reach the stabilization phase within 30 min. The reaction rate of RB extract for AgNP synthesis was determined by plotting $\ln [a/(1-a)]$ versus time (where $a = [A(t)/A(\infty)]$; $A(t)$ and $A(\infty)$ are the absorbance at time t and ∞, respectively) [43, 44]. The rate constant (k_{obs}) of the reaction was 0.210 min^{-1} (inset in Figure 2(c)). Therefore, the results indicated the optimized irradiation time of 30 min.

3.1.2. Effect of Irradiation Time on the AgNP Synthesis. Based on the kinetic reaction, the influence of irradiation time on the size and morphology of AgNP was investigated for 30 min as shown in Figure 3. The formation of AgNPs was initially identified by changing the solution color from light brown to dark brown with increasing sunlight irradiation time from 5 to 30 min (Figure 3(b)). As shown in Figure 3(a), the intensity of UV–vis absorption spectra increased over an increasing irradiation time, indicating the formation of AgNPs. The slight change of absorption peak was consistent with the SEM results that the mean particle size demonstrated a small decrease from 62.34 ± 1.00 to 59.48 ± 0.37 nm with an increase irradiation time from 5 to 30 min. As illustrated in Figure 3(d), the symmetrical narrow range of size distribution could be observed with the synthesized AgNPs after irradiation for 30 min. Moreover, approximately 50% of total particle synthesis for 30 min was distributed in the narrow range between 55 and 65 nm. It has been reported that the particle size and shape of AgNPs synthesized by light-assisted technique could be controlled by wavelength(s) of light and irradiation time [45, 46]. However, the irradiation time used in this study obtained a similar shape of AgNPs (Figure 3(c)).

3.1.3. Effect of the Volume Ratio of $AgNO_3$ to RB Solution on the AgNP Synthesis. The effect of the volume ratio of $AgNO_3$ to RB solution was performed at six different proportions. An increase of RB volume changed color of AgNP solutions from light red to dark red (Figure 4(b)). As demonstrated in the UV–vis spectra (Figure 4(a)), when the volume ratio of extracted RB solution was reduced from 10 to 1, the absorption peaks showed a decreasing intensity. In addition, the surface plasmon peaks were shifted towards shorter wavelengths from 500 to 400 nm. This result indicated a reduction in the mean diameter of AgNPs [47]. However, it should be noted that the UV–vis extinction spectra including the shifting intensity, and the full width of absorption peaks, were positively related to not only size but also size distribution and shape of AgNPs [48].

SEM images of the synthesized AgNPs are displayed in Figure 4(c). All synthesized AgNPs demonstrated the spherical morphology, and the agglomerated particles could be observed in all conditions. As shown in Figure 4(d), the size of AgNPs was decreased from 68.49 ± 1.01 to 37.98 ± 0.85

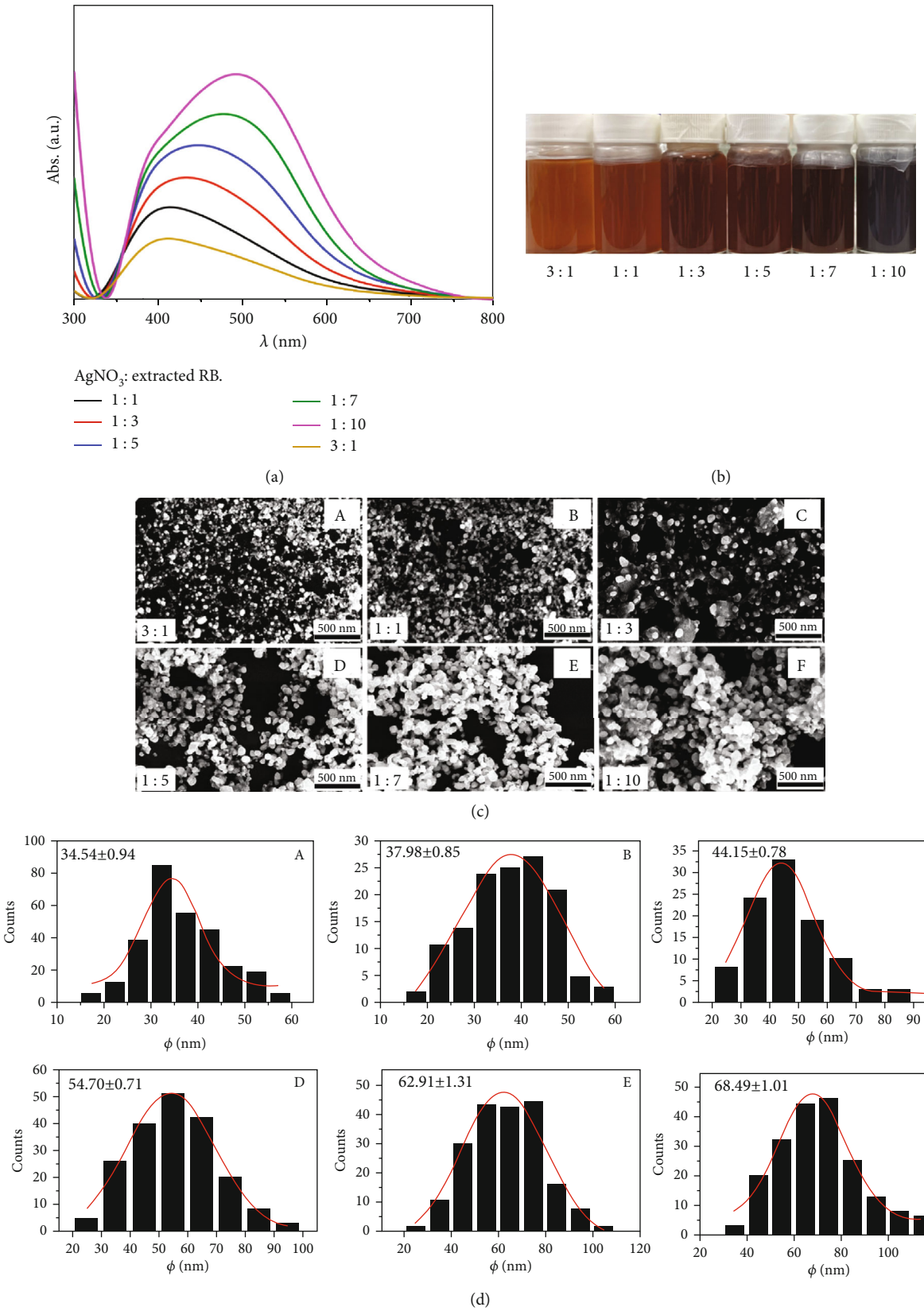

Figure 4: Effect of volume ratios of $AgNO_3$ to RB extract: A 3 : 1, B 1 : 1, C 1 : 3, D 1 : 5, E 1 : 7, and F 1 : 10 (pH 2.5, 30 min irradiation) on the characteristics of AgNPs: (a) UV–vis spectra, (b) the color of AgNPs dispersed in solution, (c) SEM images, and (d) particle size distribution.

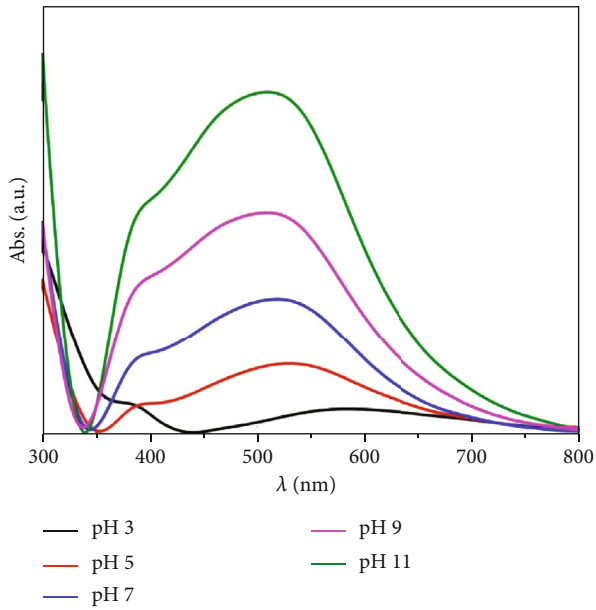

(a)

(b)

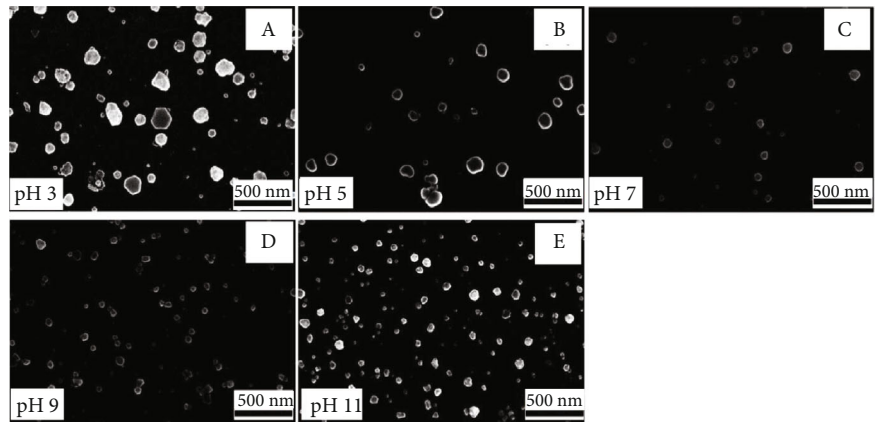

(c)

Figure 5: Continued.

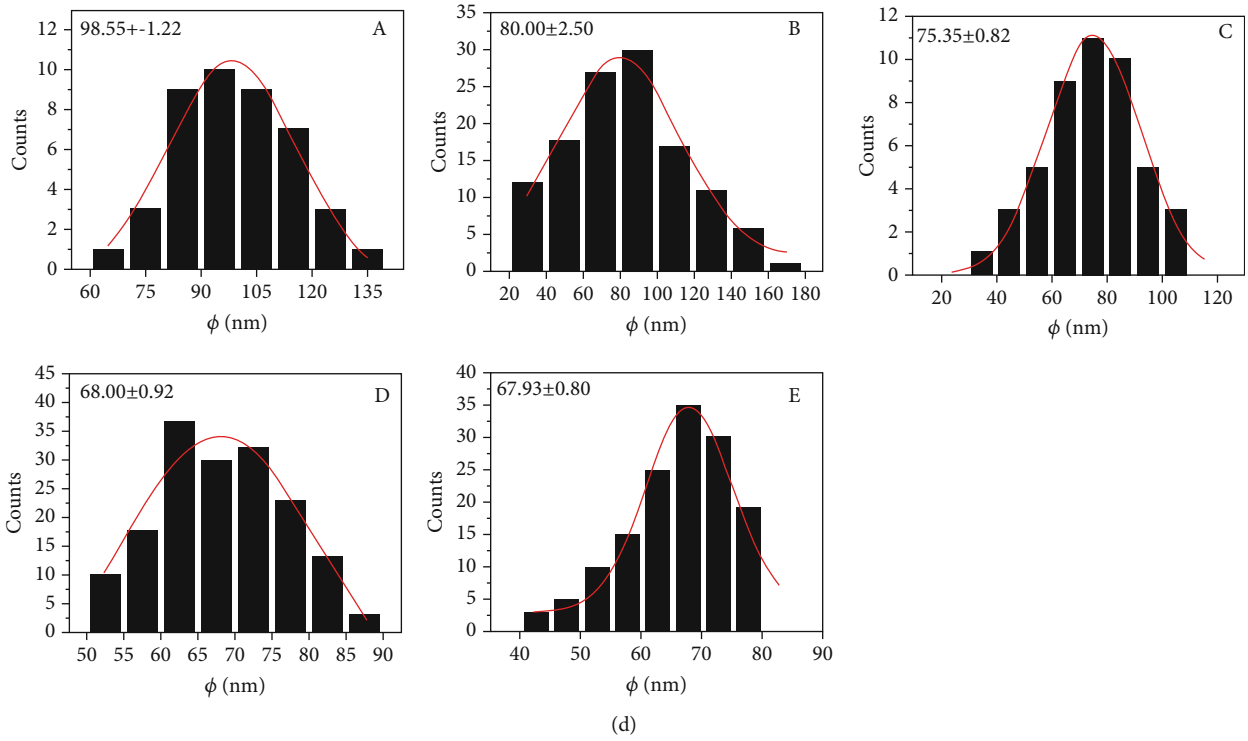

Figure 5: Effect of different pH values: A pH 3, B pH 5, C pH 7, D pH 9, and E pH 11 ($AgNO_3$: RB extract 1 : 12.5, 30 min irradiation) on the characteristics of AgNPs: (a) UV–vis spectra, (b) the color of AgNPs dispersed in solution, (c) SEM images, and (d) particle size distribution.

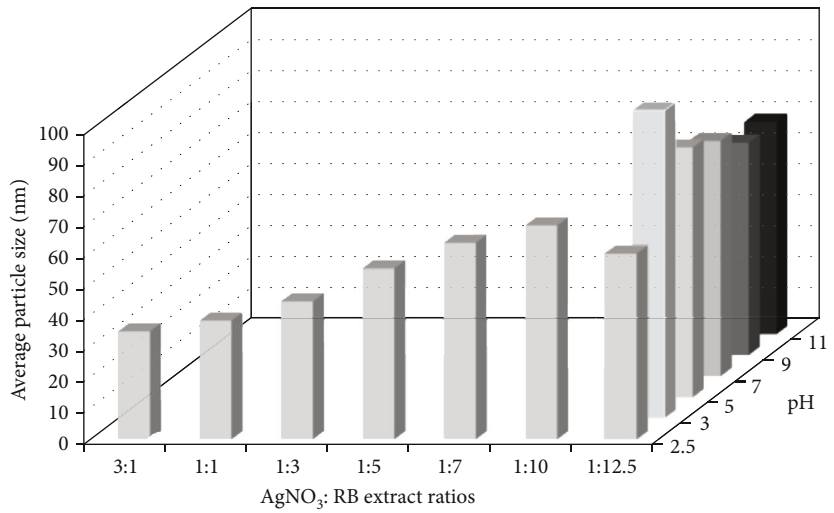

Figure 6: Effects of different pH values and different ratios of $AgNO_3$: RB extract on the average size of AgNPs.

nm, and the particles were distributed in a narrow range when the volume ratio of RB solution was reduced from 10 to 1. This finding was in agreement with the blue-shifted UV–vis spectra. However, when the volume ratio of $AgNO_3$ to RB extract was increased from 1 : 1 to 3 : 1, the results showed a slight decrease of particle size from 37.98 ± 0.85 to 34.54 ± 0.94 nm, implying the limited capacity of reducing agents in RB extract. This finding was consistent with the previous study of Jain and Mehata [49] that the size of AgNPs could be increased by increasing a volume ratio of leaf extracts of *Ocimum sanctum* or quercetin, which is a polyphenolic flavonoid.

3.1.4. Effect of pH on the AgNP Synthesis. AgNPs synthesized by using RB extract were performed over a pH range of 3–11. Figure 5(a) demonstrates the UV–visible spectra of AgNP formation. The intensity of absorbance peaks was increased with increasing pH from 3 to 11. The blue-shift wavelength was also observed with an increase of pH condition and indicated the larger size of AgNPs in the acidic medium than in

Table 1: AgNPs synthesized by RB extract in comparison with different rice variety, plant part, and techniques.

Rice variety	Part	Synthesis techniques	Synthesized conditions	Characteristics of AgNPs Particle size (nm)	Shape
RB	Grain	Plant-based-reducing agent under photoirradiation	(1) $AgNO_3$ (50 mM) to the extract (0.1% *w*/*w*) ratio of 1 : 12.5 (2) Room temperature under 1 sun (3) Reaction time 30 min (4) pH 2.5 (crystalline form)	59.48 ± 0.37 (measurement based on SEM images)	Sphere and hexagon
RNR-15048 [34]	Leaf	Plant-based-reducing agent with autoclaving	(1) $AgNO_3$ (0.6 mM) to the extract (0.4%) (2) Temperature 121°C under autoclaving condition (3) Reaction time 30 min (4) pH: no data	110.8 (measured using a zeta sizer)	Sphere
Jasmine rice [33]	Bran Husk Germ	Plant-based-reducing agent	(1) $AgNO_3$ (0.1 M) to the extract ratio of 100 : 1 (2) Temperature 75°C (3) Reaction time 60 min (4) pH: no data	>346.4 ± 36.8 (measured using a dynamic light scattering analyzer)	No data
Japonica, Kaohsiung 145 [35]	Husk	Plant-based-reducing agent	(1) $AgNO_3$ (0.001 M) to the extract ratio of 10 : 1 (2) Temperature 25°C (3) Reaction time 60 min (4) pH 10	<15 (measurement based on TEM images)	Sphere

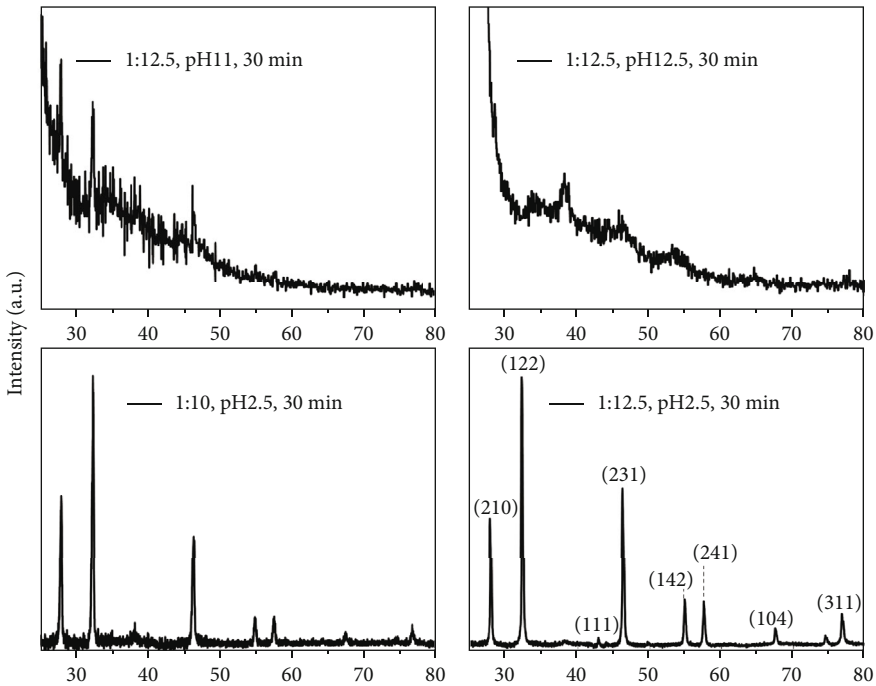

Figure 7: XRD patterns of AgNPs derived from various synthesis conditions.

the alkaline medium. In accordance with Figure 5(b), the color of AgNP solutions was also changed from light brown to dark red-brown color with increasing pH from 3 to 11. It should be noted that the color of the AgNP solution provided a convenient spectroscopic signature relating to the effect of pH on nanoparticle formation. In addition, the SEM images confirmed that the particles produced in all pH conditions were in nanometer size in different shapes including hexagonal and spherical shape (Figure 5(c)).

As demonstrated in Figure 5(d), it was clear that the mean particle size of AgNPs was decreased from 98.55 ± 1.22 to 67.93 ± 0.80 nm when the pH of reaction was increased from 3 to 11. Additionally, the particle sizes synthesized in acidic conditions (pH 3 and 5) were distributed in a wider range (20–180 nm) than those in basic conditions (pH 9 and 11; 40–90 nm) (as shown in Figure 5(d)). These results indicated that the alkaline pH medium enhanced the reducing and stabilizing capability of the polyphenolic compounds in RB extract. The reaction pH could influence the pKa and electrical charges of phenolic molecules, which affects the capping and stabilizing abilities and subsequently the growth of the nanoparticles [50]. At alkaline pH, a number of electron-donating groups (–OH) of phenol molecules in RB extract were more deprotonated and facilitated a higher number of Ag^+ ions to bind and subsequently obtained AgNPs with smaller diameters than those synthesized in an acidic environment. Because polyphenolic compounds including flavonoids and tannins [51] are known to be major secondary metabolites of several plants, the effect pH on the synthesis of metal NPs was similarly reported by using a reducer from *Terminalia chebula* fruit [52], olive leaf [50], and oak fruit hull extracts [53].

It should be noted that the irradiation time has small effect on the particle size of AgNPs, compared with the effect of volume ratio and pH. Therefore, the effect of volume ratio and pH is plot against the average particle size of AgNPs (as illustrated in Figure 6). The AgNPs in the synthesis condition at pH 2.5 showed the smallest size, although the trend of particle size was increased with a decreasing pH solution from 11 to 3. The nonlinear relationship between pH and the particle size could be similarly observed in the synthesis of AgNPs using herbal extract [54, 55]. This could be related to different charged surface on NPs in different pH [55, 56]. By fixing the solution pH at 2.5, a varied volume ratio of RB extract obtained the smaller size of AgNPs in comparison with other pH conditions (Figure 6). However, the ratio of 1 : 12.5 ($AgNO_3$: RB extract) obtained a slightly decreasing particle size (approximately 60 nm), comparing with the lower ratios of 1 : 7 and 1 : 10 (about 63 and 69 nm, respectively). This result is consistent with the synthesized AgNPs by tannic acid in polyol reaction [57]. The average size of AgNPs was decreased from 23 to17 nm with increasing concentration of tannic acid of from 10 to 100 μM due to the accelerated reduction of Ag^+ by tannic acid [57–59]. However, tannic acid at a very high concentration of 1000 μM obtained a large particle size of 85 nm because the reduction of Ag^+ was decelerated by the chelation ability of tannic acid [57–59]. Moreover, the effect of plant extraction ratios on the AgNP synthesis resulted from the overall chemical reaction. One phytomolecule can perform dual functions as reducing and capping agents to contribute AgNPs, and some of them can induce the opposite effects on the synthesis reaction depending on the concentration [57]. Therefore, the desired size of particles was appropriately adjusted by varying RB extract ratios.

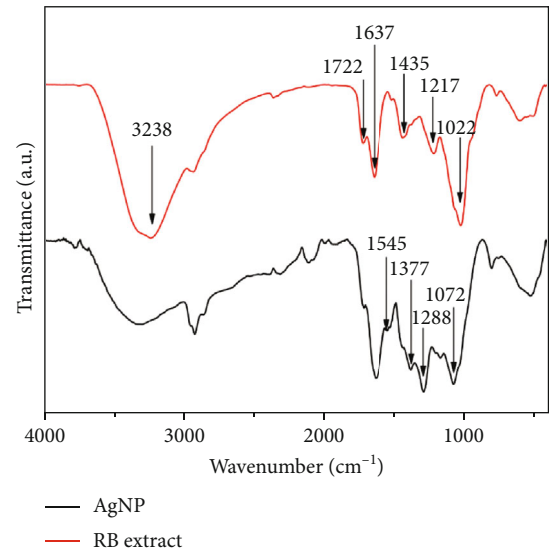

Figure 8: FT-IR spectra of RB extract and AgNPs derived by RB extract.

The comparison with the previous methods using rice extract for AgNP synthesis is shown in Table 1.This study presents a rapid and effective combination approach to synthesize AgNPs with sub-100-nm-sized spherical and hexagonal particles within 30 min at room temperature by using a ratio of $AgNO_3$ to RB extract 1 : 12.5 at pH 2.5, whereas the condition of previous reports required a high temperature (75 and 121°C) or a long reaction time (60 min) for synthesis.

3.2. XRD. The selected AgNPs, which were obtained from the conditions providing the high UV-visible peak intensity results, were investigated the crystallinity by XRD. The crystal phase structure of AgNPs prepared with different synthesis conditions was investigated by XRD (Figure 7). The characteristic peaks of metallic silver constructed with face-centered (fcc) cubic structure JCPDS (Card no. 04–0783) were observed in the sample prepared with $AgNO_3$: RB extract volume ratio of 1 : 12.5 at pH 2.5 with 30 min irradiation. The peaks at 27.84°, 32.24°, 38.12°, 46.24°, 54.84°, 67.46°, and 76.74° showed the characteristic peaks of metallic Ag crystal which can be indexed to (210), (122), (111), (231), (142), (241), (104), and (311), respectively [60]. This clearly confirms that a pure crystalline structure of AgNPs was successfully prepared by using RB extract. In addition, the XRD pattern of AgNPs synthesized using high pH conditions exhibited amorphous structures. We assume that the growth rate of AgNPs is very fast, leading to the formation of a non-ordered crystal structure inside the lattice of Ag particles. On the other hand, the growth rate of Ag crystal in acidic condition (low pH) is well-controlled to form crystal structure. The average crystallite size of synthesized AgNPs was evaluated

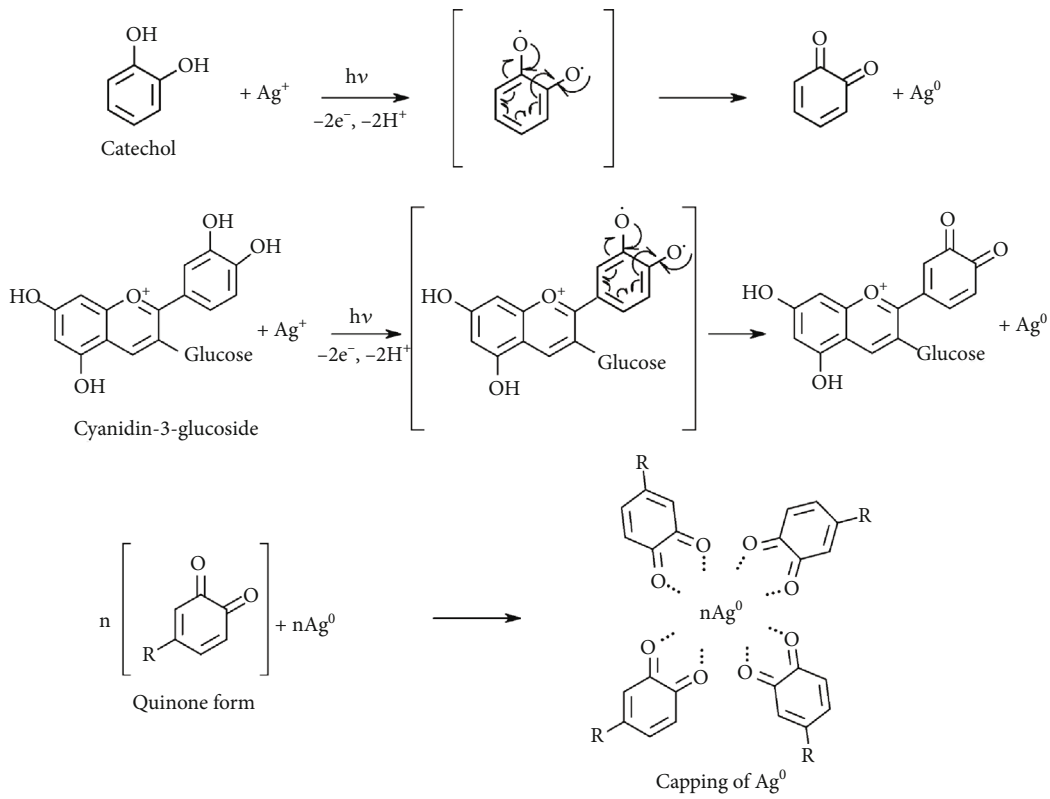

Figure 9: Schematic illustration of proposed mechanism of biosynthesized AgNPs by phytochemical constituents in RB extract [44, 72].

by using Scherrer's formula. The average crystallite size of AgNPs synthesized at ratio of 1 : 10, pH 2.5 for 30 min was 27.48 nm, whereas the average crystallite size of AgNPs synthesized at ratio of 1 : 12.5, and pH 2.5 for 30 min was 36.47 nm.

3.3. FT-IR. FT-IR has been conducted to investigate functional groups of RB extract and formation mechanism of AgNPs. From Figure 8, IR spectrum of RB extract exhibited broad absorption band at 3300–3200 cm^{-1} that correlates to hydroxyl (OH) stretching of phenolic component and amide (NH) stretching of protein component. The major peaks at 1722, 1637, 1435, 1217, and 1022 cm^{-1} are corresponded to C=O stretching of carbonyl group, conjugated C=C or amide I, CH_2 bending vibrations, C–O–C, and C–OH vibration, respectively [61–64]. For FT-IR spectrum of synthesized AgNPs, it was clearly seen that the OH absorption band at 3300–3200 cm^{-1} region was decreased, while the C=O signal was enhanced. This indicated that the OH of phenolic compounds in RB extract were involved in reducing process to form metallic Ag capped with carbonyl functionality. In addition, new absorption peaks at 1545, 1377, 1288, and 1072 cm^{-1} were observed. These peaks could be assigned to amide II stretching, C–N stretching, and C–O–C vibration characteristic, suggesting that ether linkage and protein in RB extract could adsorb on the surface of AgNPs [65–67].

Based on the Folin-Ciocalteu assay, RB extract in this study contained phenolic compounds approximately 13 mg GAE/g. It has been reported that the top three phenolic compounds found in Thai RB extract included 2-methoxy-vinyl phenol, catechol, and guaiacol [32]. Besides, the documented anthocyanidins in RB extract were cyanidin-3-glucoside and peonidin-3-O-glucoside [68]. Together with the result of FT-IR spectra, the proposed mechanism of biosynthesized AgNPs by phytochemical constituents in RB extract is illustrated in Figure 9. The oxidation of these compounds causes the formation of phenoxy radicals, which their electrons can be delocalized by resonance along with reducing the Ag^+ ion to form AgNPs [69, 70]. Additionally, this resonance did not only contribute to the stabilized phenoxy radicals of phenolic acid but also could possibly prevent the coagulation of prepared metal silver nuclei [44, 69]. Apart from the phenolic constituents, RB bran extract was reported to have protein content [71]; therefore, it could be notified that the amino acid may also serve as reducing and stabilizing agents similar to the phenolic compounds.

3.4. Antibacterial Activity of the Synthesized AgNPs. The antibacterial activity of the synthesized AgNPs using different conditions was assessed through the disc diffusion method against Gram-positive *S. aureus* and Gram-negative *E. coli*. The antibacterial activity was clearly observed in the $AgNO_3$ solution (a positive control) and AgNP samples. Conversely, the sterile DI water, which was used as a negative control, showed no antibacterial activity as shown by no inhibition zone (Figure 10). As presented in Figures 10(a)–10(c), the inhibition zones of the synthesized AgNPs at different conditions against *S. aureus* (9.17 ± 0.58 to 10.38 ± 0.25 mm) were significantly higher ($p < 0.05$) than those against *E. coli*. (6.83 ± 0.29 to 7.50 ± 0.50 mm). These results clearly

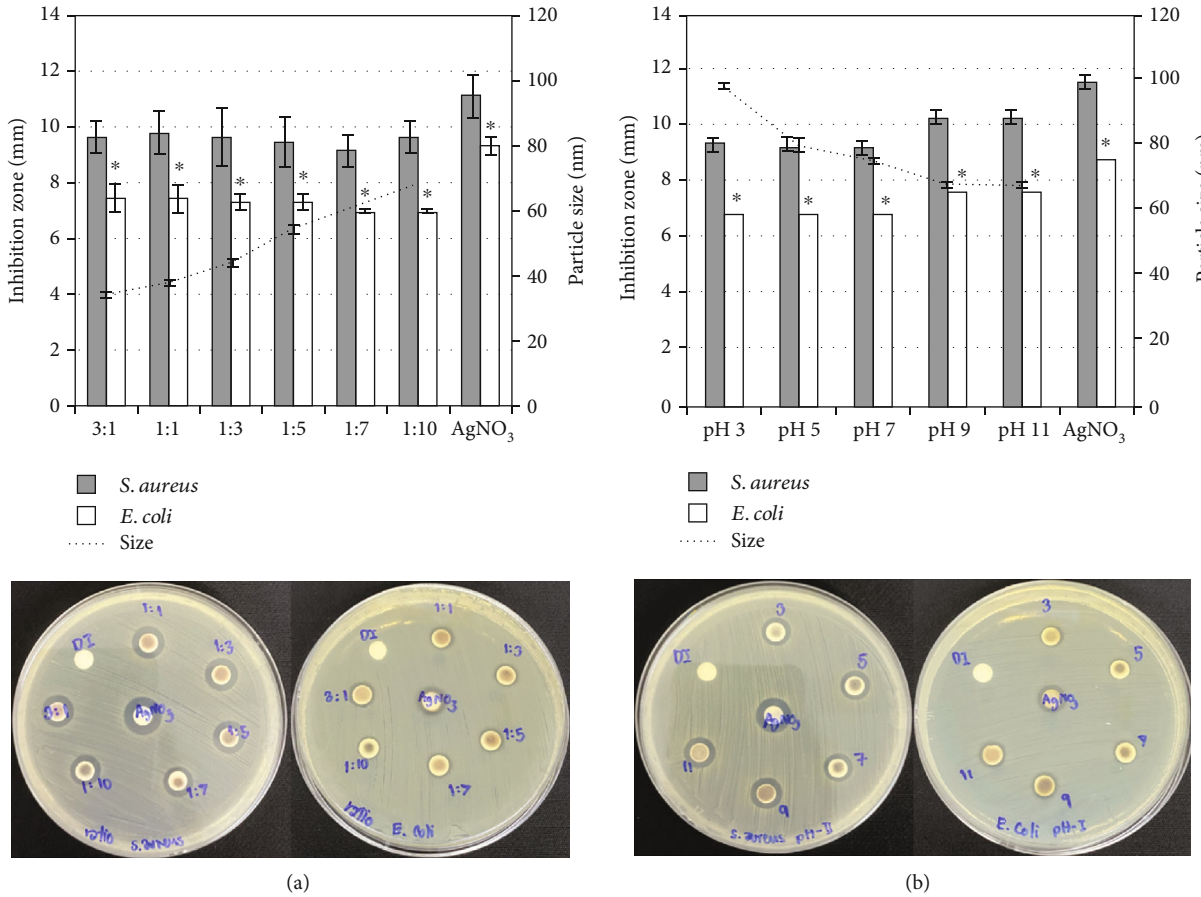

(a) (b)

Figure 10: Continued.

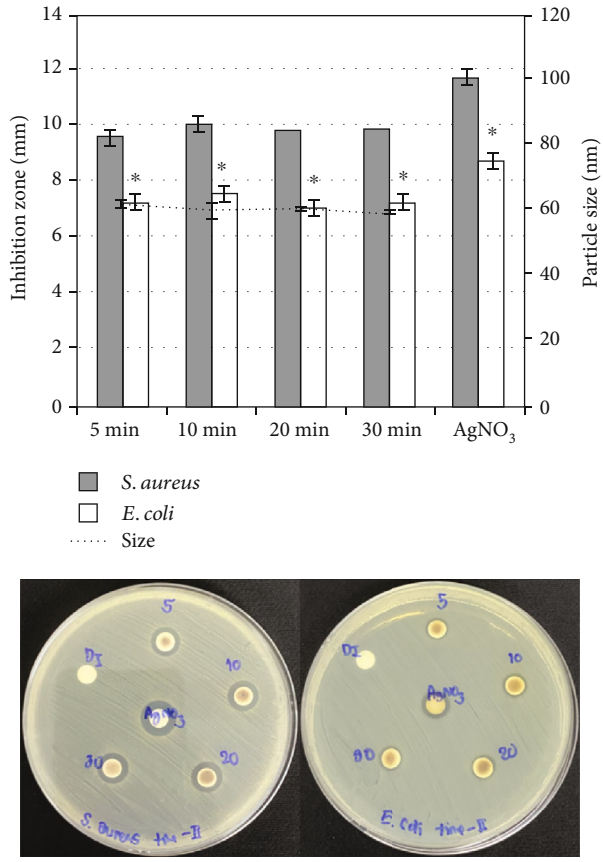

(c)

Figure 10: Inhibition zones of AgNPs obtained from various conditions of (a) volume ratios of $AgNO_3$ to RB extract (pH 2.5, 30 min irradiation), (b) pH ($AgNO_3$: RB; 1 : 12.5, 30 min irradiation), and (c) irradiation times ($AgNO_3$: RB; 1 : 12.5, pH 2.5) against *S. aureus* and *E. coli* compared with the mean of particle size. Each symbol indicates the mean ± S.D. ($n = 3$). *Significant difference between Gram-positive and Gram-negative bacteria ($p < 0.05$).

indicated that the synthesized AgNPs using RB extract exhibited more effective antibacterial activity against Gram-positive bacteria than against Gram-negative bacteria, which were in agreement with the previous studies of Khalil et al. [50], Huong and Nguyen [73], and Jemilugba et al. [74]. In addition, it could be noted that the smaller size of AgNPs provided the larger inhibition zone as obviously shown in Figure 10(b). Because AgNPs would attach to the bacterial cell membrane and release silver ions to penetrate and interact with biomolecule and DNA, the smaller size of NPs, the higher surface area to volume ratio of NPs could lead to more attachment and stronger binding to the cell membrane, resulting in the higher efficacy [75, 76]. On the other hand, several studies have reported that AgNPs were more susceptible to Gram-negative bacteria than Gram-positive bacteria [77, 78]. This phenomenon may be caused by the different membrane structure of the microorganism. Due to the thick layer of peptidoglycan in Gram-positive bacteria, it makes them more rigid and makes them less permeable for the silver ions to get inside the cells [79]. However, the opposed antibacterial susceptibility of AgNPs on Gram-negative and Gram-positive bacteria could be affected by the different physicochemical properties of AgNPs, which played a critical effect on their antibacterial potential including shape, size, surface charge, and concentrations [36, 80]. Mandal et al. [81] reported that Gram-positive *Enterococcus faecalis* cells accumulated more Ag^+ ions than Gram-negative *Proteus vulgaris* as shown by the lower zeta potential of −15 and −26 mV, respectively, which indicated the preferentially eradicated Gram-positive bacteria and the charge-dependent mechanism of AgNP efficacy. In addition, AgNPs in the spherical shape were effective against both Gram-positive and Gram-negative bacterial than the rod shape as shown by the lower minimum inhibitory concentrations [82]. Because AgNPs in the spherical shape has larger effective specific contact area as compared to the rod shape, they could achieve closer contact with bacterial cell and causes more damages [83]. So, the antibacterial efficacy of light-assisted AgNPs using RB extracts was based on the bacteria strain and the size of AgNPs. Apart from effective inhibition of susceptible bacteria, AgNPs could inhibit the formation of bacterial biofilm, which is one of the virulence factors of resistant bacteria [84]. Therefore, their antibacterial activity of AgNPs on multidrug resistant bacteria in both standard and clinical isolates, and antibiofilm formation are deserved for further investigation.

4. Conclusions

The utilization of RB extract as a reductant and a stabilizer assisted with photoirradiation was the efficient and rapid approach for AgNP synthesis. This method was able to complete the synthesis in 30 min with a rate constant of $0.210\,min^{-1}$. The average size of the AgNP was adjustable by changing the synthesis parameters. The high volume of RB extract and the acidic pH condition could obtain the small size of crystalline AgNPs. The synthesized AgNPs also demonstrated the effective antibacterial activity against both Gram-positive and Gram-negative bacteria. Therefore, the photoassisted synthesis of AgNPs using RB extract is valuable for a green production of nanomaterials used in biomedical-related applications.

Data Availability

The authors declare that all data supporting the findings in this study are provided in the results and discussion section within the article.

Conflicts of Interest

The authors declare no conflict of interest.

Acknowledgments

Dr. Karn Wongsariya, Faculty of Science, King Mongkut's Institute of Technology Ladkrabang, is gratefully acknowledged for providing bacterial strains. This research was funded by the King Mongkut's Institute of Technology Ladkrabang Research Fund, grant number KREF186220. This research was also partially supported by the National Research Council of Thailand (NRCT).

References

[1] S. Guo and E. Wang, "Noble metal nanomaterials: controllable synthesis and application in fuel cells and analytical sensors," *Nano Today*, vol. 6, no. 3, pp. 240–264, 2011.

[2] R. J. Peters, H. Bouwmeester, S. Gottardo et al., "Nanomaterials for products and application in agriculture, feed and food," *Trends in Food Science & Technology*, vol. 54, pp. 155–164, 2016.

[3] G. Fytianos, A. Rahdar, and G. Z. Kyzas, "Nanomaterials in cosmetics: recent updates," *Nanomaterials*, vol. 10, no. 5, p. 979, 2020.

[4] P. J. Rivero, A. Urrutia, J. Goicoechea, and F. J. Arregui, "Nanomaterials for functional textiles and fibers," *Nanoscale research letters*, vol. 10, no. 1, p. 501, 2015.

[5] S. Wanwong, W. Sangkhun, S. Z. Homayounfar, K.-W. Park, and T. L. Andrew, "Wash-stable, oxidation resistant conductive cotton electrodes for wearable electronics," *RSC Advances*, vol. 9, no. 16, pp. 9198–9203, 2019.

[6] O. V. Salata, "Applications of nanoparticles in biology and medicine," *Journal of nanobiotechnology*, vol. 2, no. 1, p. 3, 2004.

[7] S. B. Yaqoob, R. Adnan, R. M. Rameez Khan, and M. Rashid, "Gold, silver, and palladium nanoparticles: a chemical tool for biomedical applications," *Frontiers in Chemistry*, vol. 8, no. 376, 2020.

[8] N. S. Wigginton, A. D. Titta, F. Piccapietra et al., "Binding of silver nanoparticles to bacterial proteins depends on surface modifications and inhibits enzymatic activity," *Environmental Science & Technology*, vol. 44, no. 6, pp. 2163–2168, 2010.

[9] S. Iravani, H. Korbekandi, S. V. Mirmohammadi, and B. Zolfaghari, "Synthesis of silver nanoparticles: chemical, physical and biological methods," *Research in pharmaceutical sciences*, vol. 9, no. 6, pp. 385–406, 2014.

[10] M. Rai, K. Kon, A. Ingle, N. Duran, S. Galdiero, and M. Galdiero, "Broad-spectrum bioactivities of silver nanoparticles: the emerging trends and future prospects," *Applied Microbiology and Biotechnology*, vol. 98, no. 5, pp. 1951–1961, 2014.

[11] A. A. Yaqoob, K. Umar, and M. N. M. Ibrahim, "Silver nanoparticles: various methods of synthesis, size affecting factors and their potential applications–a review," *Applied Nanoscience*, vol. 10, no. 5, pp. 1369–1378, 2020.

[12] M. A. Hussain, A. Shah, I. Jantan et al., "One pot light assisted green synthesis, storage and antimicrobial activity of dextran stabilized silver nanoparticles," *Journal of nanobiotechnology*, vol. 12, no. 1, p. 53, 2014.

[13] M. G. Guzmán, J. Dille, and S. Godet, "Synthesis of silver nanoparticles by chemical reduction method and their antibacterial activity," *International Journal of Chemical and Biomolecular Engineering*, vol. 2, no. 3, pp. 104–111, 2009.

[14] S. F. Adil, M. E. Assal, M. Khan, A. Al-Warthan, M. R. H. Siddiqui, and L. M. Liz-Marzán, "Biogenic synthesis of metallic nanoparticles and prospects toward green chemistry," *Dalton Transactions*, vol. 44, no. 21, pp. 9709–9717, 2015.

[15] S. Tharani, D. Bharathi, and R. Ranjithkumar, "Extracellular green synthesis of chitosan-silver nanoparticles using Lactobacillus reuteri for antibacterial applications," *Biocatalysis and Agricultural Biotechnology*, vol. 30, p. 101838, 2020.

[16] H. Peng, A. Yang, and J. Xiong, "Green, microwave-assisted synthesis of silver nanoparticles using bamboo hemicelluloses and glucose in an aqueous medium," *Carbohydrate Polymers*, vol. 91, no. 1, pp. 348–355, 2013.

[17] X. Li, H. Xu, Z.-S. Chen, and G. Chen, "Biosynthesis of nanoparticles by microorganisms and their applications," *Journal of Nanomaterials*, vol. 2011, 16 pages, 2011.

[18] M. Khan, M. R. Shaik, S. F. Adil et al., "Plant extracts as green reductants for the synthesis of silver nanoparticles: lessons from chemical synthesis," *Dalton Transactions*, vol. 47, no. 35, pp. 11988–12010, 2018.

[19] Y. Y. Loo, B. W. Chieng, M. Nishibuchi, and S. Radu, "Synthesis of silver nanoparticles by using tea leaf extract from Camellia sinensis," *International Journal of Nanomedicine*, vol. 7, p. 4263, 2012.

[20] M. A. Ali, T. Ahmed, W. Wu et al., "Advancements in plant and microbe-based synthesis of metallic nanoparticles and their antimicrobial activity against plant pathogens," *Nanomaterials*, vol. 10, no. 6, 2020.

[21] M. Kitching, M. Ramani, and E. Marsili, "Fungal biosynthesis of gold nanoparticles: mechanism and scale up," *Microbial Biotechnology*, vol. 8, no. 6, pp. 904–917, 2015.

[22] J. J. Vijaya, N. Jayaprakash, K. Kombaiah et al., "Bioreduction potentials of dried root of Zingiber officinale for a simple green synthesis of silver nanoparticles: antibacterial studies," *Journal*

of Photochemistry and Photobiology B: Biology, vol. 177, pp. 62–68, 2017.

[23] D. Bharathi, M. D. Josebin, S. Vasantharaj, and V. Bhuvaneshwari, "Biosynthesis of silver nanoparticles using stem bark extracts of Diospyros montana and their antioxidant and antibacterial activities," *Journal of Nanostructure in Chemistry*, vol. 8, no. 1, pp. 83–92, 2018.

[24] M. Asimuddin, M. R. Shaik, N. Fathima et al., "Study of antibacterial properties of Ziziphus mauritiana based green synthesized silver nanoparticles against various bacterial strains," *Sustainability*, vol. 12, no. 4, p. 1484, 2020.

[25] D. Bharathi and V. Bhuvaneshwari, "Evaluation of the cytotoxic and antioxidant activity of phyto-synthesized silver nanoparticles using Cassia angustifolia flowers," *BioNanoScience*, vol. 9, no. 1, pp. 155–163, 2019.

[26] D. Bharathi, S. Vasantharaj, and V. Bhuvaneshwari, "Green synthesis of silver nanoparticles using Cordia dichotoma fruit extract and its enhanced antibacterial, anti-biofilm and photo catalytic activity," *Materials Research Express*, vol. 5, no. 5, article 055404, 2018.

[27] D. Sunita, D. Tambhale, V. Parag, and A. Adhyapak, "Facile green synthesis of silver nanoparticles using Psoralea corylifolia. Seed extract and their in-vitro antimicrobial activities," *International Journal of Pharmacy and Biological Sciences*, vol. 5, no. 1, pp. 457–467, 2014.

[28] N. Tarannum and Y. K. Gautam, "Facile green synthesis and applications of silver nanoparticles: a state-of-the-art review," *RSC Advances*, vol. 9, no. 60, pp. 34926–34948, 2019.

[29] C. N. Nandana, M. Christeena, and D. Bharathi, "Synthesis and characterization of chitosan/silver nanocomposite using rutin for antibacterial, antioxidant and photocatalytic applications," *Journal of Cluster Science*, vol. 82, pp. 1–11, 2021.

[30] V. Leardkamolkarn, W. Thongthep, P. Suttiarporn, R. Kongkachuichai, S. Wongpornchai, and A. Wanavijitr, "Chemopreventive properties of the bran extracted from a newly-developed Thai rice: the Riceberry," *Food Chemistry*, vol. 125, no. 3, pp. 978–985, 2011.

[31] P. Prangthip, R. Surasiang, R. Charoensiri et al., "Amelioration of hyperglycemia, hyperlipidemia, oxidative stress and inflammation in steptozotocin-induced diabetic rats fed a high fat diet by riceberry supplement," *Journal of Functional Foods*, vol. 5, no. 1, pp. 195–203, 2013.

[32] P. Suttiarporn, P. Sookwong, and S. Mahatheeranont, "Fractionation and identification of antioxidant compounds from bran of Thai black rice cv. Riceberry," *International Journal of Chemical Engineering and Applications*, vol. 7, no. 2, p. 109, 2016.

[33] T. Suwan, S. Khongkhunthian, and S. Okonogi, "Green synthesis and inhibitory effects against oral pathogens of silver nanoparticles mediated by rice extracts," *Drug discoveries & therapeutics*, vol. 12, no. 4, pp. 189–196, 2018.

[34] A. J. Kora, J. Mounika, and R. Jagadeeshwar, "Rice leaf extract synthesized silver nanoparticles: an in vitro fungicidal evaluation against Rhizoctonia solani, the causative agent of sheath blight disease in rice," *Fungal Biology*, vol. 124, no. 7, pp. 671–681, 2020.

[35] Y.-S. Liu, Y.-C. Chang, and H.-H. Chen, "Silver nanoparticle biosynthesis by using phenolic acids in rice husk extract as reducing agents and dispersants," *Journal of Food and Drug Analysis*, vol. 26, no. 2, pp. 649–656, 2018.

[36] A. Kędziora, M. Speruda, E. Krzyżewska, J. Rybka, A. Łukowiak, and G. Bugla-Płoskońska, "Similarities and differences between silver ions and silver in nanoforms as antibacterial agents," *International journal of molecular sciences*, vol. 19, no. 2, p. 444, 2018.

[37] M. Zaier, L. Vidal, S. Hajjar-Garreau, and L. Balan, "Generating highly reflective and conductive metal layers through a light-assisted synthesis and assembling of silver nanoparticles in a polymer matrix," *Scientific Reports*, vol. 7, no. 1, pp. 1–10, 2017.

[38] H. S. Toh, R. L. Faure, L. B. M. Amin, C. Y. F. Hay, and S. George, "A light-assisted in situ embedment of silver nanoparticles to prepare functionalized fabrics," *Nanotechnology, science and applications*, vol. 10, p. 147, 2017.

[39] M. Jayapriya, D. Dhanasekaran, M. Arulmozhi, E. Nandhakumar, N. Senthilkumar, and K. Sureshkumar, "Green synthesis of silver nanoparticles using Piper longum catkin extract irradiated by sunlight: antibacterial and catalytic activity," *Research on Chemical Intermediates*, vol. 45, no. 6, pp. 3617–3631, 2019.

[40] F. Chutrakulwong, K. Thamaphat, and P. Limsuwan, "Photo-irradiation induced green synthesis of highly stable silver nanoparticles using durian rind biomass: effects of light intensity, exposure time and pH on silver nanoparticles formation," *Journal of Physics Communications*, vol. 4, no. 9, article 095015, 2020.

[41] V. L. Singleton, R. Orthofer, and R. M. Lamuela-Raventós, "[14] Analysis of total phenols and other oxidation substrates and antioxidants by means of folin-ciocalteu reagent," *Methods in Enzymology*, vol. 299, pp. 152–178, 1999.

[42] P. Jiamboonsri, P. Pithayanukul, R. Bavovada, and M. T. Chomnawang, "The inhibitory potential of Thai mango seed kernel extract against methicillin-resistant Staphylococcus aureus," *Molecules*, vol. 16, no. 8, pp. 6255–6270, 2011.

[43] E. Priyadarshini and N. Pradhan, "Metal-induced aggregation of valine capped gold nanoparticles: an efficient and rapid approach for colorimetric detection of Pb^{2+} ions," *Scientific Reports*, vol. 7, no. 1, pp. 1–8, 2017.

[44] M. K. Choudhary, J. Kataria, and S. Sharma, "Evaluation of the kinetic and catalytic properties of biogenically synthesized silver nanoparticles," *Journal of Cleaner Production*, vol. 198, pp. 882–890, 2018.

[45] H. Jia, W. Xu, J. An, D. Li, and B. Zhao, "A simple method to synthesize triangular silver nanoparticles by light irradiation," *Spectrochimica Acta Part A: Molecular and Biomolecular Spectroscopy*, vol. 64, no. 4, pp. 956–960, 2006.

[46] A. Callegari, D. Tonti, and M. Chergui, "Photochemically grown silver nanoparticles with wavelength-controlled size and shape," *Nano Letters*, vol. 3, no. 11, pp. 1565–1568, 2003.

[47] M. Ider, K. Abderrafi, A. Eddahbi, S. Ouaskit, and A. Kassiba, "Silver metallic nanoparticles with surface plasmon resonance: synthesis and characterizations," *Journal of Cluster Science*, vol. 28, no. 3, pp. 1051–1069, 2017.

[48] M. Chen, Y.-G. Feng, X. Wang, T.-C. Li, J.-Y. Zhang, and D.-J. Qian, "Silver nanoparticles capped by oleylamine: formation, growth, and self-organization," *Langmuir*, vol. 23, no. 10, pp. 5296–5304, 2007.

[49] S. Jain and M. S. Mehata, "Medicinal plant leaf extract and pure flavonoid mediated green synthesis of silver nanoparticles and their enhanced antibacterial property," *Scientific Reports*, vol. 7, no. 1, pp. 1–13, 2017.

[50] M. M. Khalil, E. H. Ismail, K. Z. El-Baghdady, and D. Mohamed, "Green synthesis of silver nanoparticles using

olive leaf extract and its antibacterial activity," *Arabian Journal of Chemistry*, vol. 7, no. 6, pp. 1131–1139, 2014.

[51] P. Jiamboonsri, P. Pithayanukul, R. Bavovada et al., "Factors influencing oral bioavailability of Thai mango seed kernel extract and its key phenolic principles," *Molecules*, vol. 20, no. 12, pp. 21254–21273, 2015.

[52] T. J. I. Edison and M. Sethuraman, "Instant green synthesis of silver nanoparticles using Terminalia chebula fruit extract and evaluation of their catalytic activity on reduction of methylene blue," *Process Biochemistry*, vol. 47, no. 9, pp. 1351–1357, 2012.

[53] R. Heydari and M. Rashidipour, "Green synthesis of silver nanoparticles using extract of oak fruit hull (Jaft): synthesis and in vitro cytotoxic effect on MCF-7 cells," *International journal of breast cancer*, vol. 2015, 6 pages, 2015.

[54] S. Wei, Y. Wang, Z. Tang et al., "A novel green synthesis of silver nanoparticles by the residues of Chinese herbal medicine and their biological activities," *RSC Advances*, vol. 11, no. 3, pp. 1411–1419, 2021.

[55] M. Riaz, V. Mutreja, S. Sareen et al., "Exceptional antibacterial and cytotoxic potency of monodisperse greener AgNPs prepared under optimized pH and temperature," *Scientific Reports*, vol. 11, no. 1, pp. 1–11, 2021.

[56] R. M. Elamawi, R. E. Al-Harbi, and A. A. Hendi, "Biosynthesis and characterization of silver nanoparticles using Trichoderma longibrachiatum and their effect on phytopathogenic fungi," *Egyptian journal of biological pest control*, vol. 28, no. 1, pp. 1–11, 2018.

[57] S. Chen, J. R. Drehmel, and R. L. Penn, "Facile synthesis of monodispersed AgNPs in ethylene glycol using mixed capping agents," *ACS Omega*, vol. 5, no. 11, pp. 6069–6073, 2020.

[58] N. G. Bastús, F. Merkoçi, J. Piella, and V. Puntes, "Synthesis of highly monodisperse citrate-stabilized silver nanoparticles of up to 200 nm: kinetic control and catalytic properties," *Chemistry of Materials*, vol. 26, no. 9, pp. 2836–2846, 2014.

[59] L. Rainville, M.-C. Dorais, and D. Boudreau, "Controlled synthesis of low polydispersity Ag@ SiO_2 core–shell nanoparticles for use in plasmonic applications," *RSC Advances*, vol. 3, no. 33, pp. 13953–13960, 2013.

[60] R. I. Priyadharshini, G. Prasannaraj, N. Geetha, and P. Venkatachalam, "Microwave-mediated extracellular synthesis of metallic silver and zinc oxide nanoparticles using macro-algae (Gracilaria edulis) extracts and its anticancer activity against human PC3 cell lines," *Applied Biochemistry and Biotechnology*, vol. 174, no. 8, pp. 2777–2790, 2014.

[61] Y. Meng, "A sustainable approach to fabricating Ag nanoparticles/PVA hybrid nanofiber and its catalytic activity," *Nanomaterials*, vol. 5, no. 2, pp. 1124–1135, 2015.

[62] M. M. I. Masum, M. M. Siddiqa, K. A. Ali et al., "Biogenic synthesis of silver nanoparticles using Phyllanthus emblica fruit extract and its inhibitory action against the pathogen Acidovorax oryzae strain RS-2 of rice bacterial brown stripe," *Frontiers in Microbiology*, vol. 10, p. 820, 2019.

[63] W. Chartarrayawadee, P. Charoensin, J. Saenma et al., "Green synthesis and stabilization of silver nanoparticles using Lysimachia foenum-graecum Hance extract and their antibacterial activity," *Green Processing and Synthesis*, vol. 9, no. 1, pp. 107–118, 2020.

[64] R. Augustine, N. Kalarikkal, and S. Thomas, "Electrospun PCL membranes incorporated with biosynthesized silver nanoparticles as antibacterial wound dressings," *Applied Nanoscience*, vol. 6, no. 3, pp. 337–344, 2016.

[65] K. Anandalakshmi, J. Venugobal, and V. Ramasamy, "Characterization of silver nanoparticles by green synthesis method using Pedalium murex leaf extract and their antibacterial activity," *Applied Nanoscience*, vol. 6, no. 3, pp. 399–408, 2016.

[66] T. Gutul, E. Rusu, N. Condur, V. Ursaki, E. Goncearenco, and P. Vlazan, "Preparation of poly(N-vinylpyrrolidone)-stabilized ZnO colloid nanoparticles," *Beilstein Journal of Nanotechnology*, vol. 5, pp. 402–406, 2014.

[67] G. Z. S. Oliveira, C. A. P. Lopes, M. H. Sousa, and L. P. Silva, "Synthesis of silver nanoparticles using aqueous extracts of Pterodon emarginatus leaves collected in the summer and winter seasons," *International Nano Letters*, vol. 9, no. 2, pp. 109–117, 2019.

[68] S. Poosri, T. Thilavech, P. Pasukamonset, C. Suparpprom, and S. Adisakwattana, "Studies on Riceberry rice (Oryza sativa L.) extract on the key steps related to carbohydrate and lipid digestion and absorption: a new source of natural bioactive substances," *NFS journal*, vol. 17, pp. 17–23, 2019.

[69] M. K. Choudhary, J. Kataria, S. S. Cameotra, and J. Singh, "A facile biomimetic preparation of highly stabilized silver nanoparticles derived from seed extract of Vigna radiata and evaluation of their antibacterial activity," *Applied Nanoscience*, vol. 6, no. 1, pp. 105–111, 2016.

[70] A. Simić, D. Manojlović, D. Šegan, and M. Todorović, "Electrochemical behavior and antioxidant and prooxidant activity of natural phenolics," *Molecules*, vol. 12, no. 10, pp. 2327–2340, 2007.

[71] P. Thamnarathip, K. Jangchud, A. Jangchud, S. Nitisinprasert, S. Tadakittisarn, and B. Vardhanabhuti, "Extraction and characterisation of Riceberry bran protein hydrolysate using enzymatic hydrolysis," *International Journal of Food Science & Technology*, vol. 51, no. 1, pp. 194–202, 2016.

[72] S. A. Al-Thabaiti and Z. Khan, "Biogenic synthesis of silver nanoparticles, sensing and photo catalytic activities for bromothymol blue," *Journal of Photochemistry and Photobiology*, vol. 3, p. 100010, 2020.

[73] V. T. Huong and N. T. Nguyen, "Green synthesis, characterization and antibacterial activity of silver nanoparticles using Sapindus mukorossi fruit pericarp extract," *Materials Today: Proceedings*, vol. 42, pp. 88–93, 2021.

[74] O. T. Jemilugba, S. Parani, V. Mavumengwana, and O. S. Oluwafemi, "Green synthesis of silver nanoparticles using Combretum erythrophyllum leaves and its antibacterial activities," *Colloid and Interface Science Communications*, vol. 31, p. 100191, 2019.

[75] Q. L. Feng, J. Wu, G. Q. Chen, F. Cui, T. Kim, and J. Kim, "A mechanistic study of the antibacterial effect of silver ions on Escherichia coli and Staphylococcus aureus," *Journal of Biomedical Materials Research*, vol. 52, no. 4, pp. 662–668, 2000.

[76] F. Raimondi, G. G. Scherer, R. Kötz, and A. Wokaun, "Nanoparticles in energy technology: examples from electrochemistry and catalysis," *Angewandte Chemie International Edition*, vol. 44, no. 15, pp. 2190–2209, 2005.

[77] Z. A. Ali, R. Yahya, S. D. Sekaran, and R. Puteh, "Green synthesis of silver nanoparticles using apple extract and its antibacterial properties," *Advances in Materials Science and Engineering*, vol. 2016, 6 pages, 2016.

[78] M. Vanaja, K. Paulkumar, G. Gnanajobitha, S. Rajeshkumar, C. Malarkodi, and G. Annadurai, "Herbal plant synthesis of antibacterial silver nanoparticles by Solanum trilobatum and its characterization," *International Journal of Metals*, vol. 2014, 8 pages, 2014.

[79] A. Abbaszadegan, Y. Ghahramani, A. Gholami et al., "The effect of charge at the surface of silver nanoparticles on antimicrobial activity against gram-positive and gram-negative bacteria: a preliminary study," *Journal of Nanomaterials*, vol. 2015, 8 pages, 2015.

[80] T. C. Dakal, A. Kumar, R. S. Majumdar, and V. Yadav, "Mechanistic basis of antimicrobial actions of silver nanoparticles," *Frontiers in Microbiology*, vol. 7, p. 1831, 2016.

[81] D. Mandal, S. K. Dash, B. Das et al., "Bio-fabricated silver nanoparticles preferentially targets Gram positive depending on cell surface charge," *Biomedicine & Pharmacotherapy*, vol. 83, pp. 548–558, 2016.

[82] D. Acharya, K. M. Singha, P. Pandey, B. Mohanta, J. Rajkumari, and L. P. Singha, "Shape dependent physical mutilation and lethal effects of silver nanoparticles on bacteria," *Scientific reports*, vol. 8, no. 1, p. 201, 2018.

[83] X. Hong, J. Wen, X. Xiong, and Y. Hu, "Shape effect on the antibacterial activity of silver nanoparticles synthesized via a microwave-assisted method," *Environmental Science and Pollution Research*, vol. 23, no. 5, pp. 4489–4497, 2016.

[84] C. Karthik, M. Chethana, H. Manukumar et al., "Synthesis and characterization of chitosan silver nanoparticle decorated with benzodioxane coupled piperazine as an effective anti-biofilm agent against MRSA: a validation of molecular docking and dynamics," *International Journal of Biological Macromolecules*, vol. 181, pp. 540–551, 2021.